# A Critical Review of Methods for Determining Stress-intensity Factors from Isochromatic Fringes

Three two-parameter methods of fracture analysis for determining the stress-intensity factor from photoelastic isochromatic-fringe data are critically reviewed by the authors

by J.M. Etheridge and J.W. Dally

ABSTRACT—Two-parameter methods of fracture analysis for determining the stress-intensity factor from photoelastic isochromatic-fringe data were critically reviewed. The methods of Irwin, Bradley and Kobayashi, and Smith were developed in detail and differences in the three approaches were noted. Theoretical fringe loops were generated for a crack of length $2a$ in a semi-infinite plate with biaxial loading. These fringe loops were used to compare the three analysis methods and to determine the accuracy of each method.

All three methods give a close estimate of the stress-intensity factor, with the Bradley-Kobayashi differencing procedure providing the most precise estimate of $K$. However, if measurement errors become excessive (larger than 2 percent) the differencing procedure magnifies these errors and the original method proposed by Irwin is the recommended approach.

The two-parameter methods can be employed to determine $K$ to within $\pm 5$ percent, provided the angle of tilt of the isochromatic-fringe loop is $73 \leqslant \theta_m < 139$ deg. If $\theta_m$ is outside this range, the two-parameter methods should not be employed.

## Introduction

Post[1] and Post and Wells[2] in the early 50's were the first investigators to show the application of photoelasticity to fracture mechanics. Irwin[3] in a discussion to Ref. 2 showed that the stress-intensity factor $K$ could be determined from a single isochromatic-fringe loop at the tip of the crack. With the Irwin method, the stress-intensity factor $K$ and a uniformly distributed stress $\sigma_{ox}$ are functions of the radius $r_m$ of the fringe loop and $\theta_m$ the angle associated with the tilt of the loop as defined in Fig. 1.

Since this work in the early 50's, Bradley and Kobayashi[4] and C.W. Smith[5] have modified Irwin's method. Bradley and Kobayashi redefined the relationship between $\sigma_{ox}$ and $K$ which resulted in a simplified relation for $K$ in terms of the fringe-loop parameters $r_m$ and $\theta_m$. Kobayashi and Bradley then introduced a differencing technique involving measurements of $\theta$ and $r$ on two fringe loops in an attempt to avoid difficulties associated with the singular terms in Irwin's solution.

Smith omitted one term in one of Irwin's equations and measured the position $r$ of the fringe loop at $\theta = \pi/2$ (along a line perpendicular to the crack extension). Smith then employed a differencing technique similar to that of Bradley and Kobayashi to uncouple $K$ and $\sigma_{ox}$ in the analysis. The data are then statistically conditioned using results from several pairs of fringes to improve the accuracy of the $K$ determination.

The primary objective of this paper is to review these three methods of analysis. The review is critical in that limitations of the two-parameter method are indicated. Also, these three methods are compared with exact theoretical results obtained for a central crack of length $2a$. Comparisons are made to show the effect of errors in the measurement of both $r_m$ and $\theta_m$.

## Two-parameter Methods of Analysis

*Irwin's Method*

Irwin[3,6] showed that the stress-intensity factor $K$ could be determined from the isochromatic-fringe loop at the tip of the crack illustrated in Fig. 1. Irwin began by writing the cartesian components of stress $\sigma_x$, $\sigma_y$ and $\tau_{xy}$ in the local neighborhood ($r << a$) of the crack tip as:

$$\begin{aligned} \sigma_x &= \frac{K}{\sqrt{2\pi r}} \cos\frac{\theta}{2} \left(1 - \sin\frac{\theta}{2} \sin\frac{3\theta}{2}\right) - \sigma_{ox} \\ \sigma_y &= \frac{K}{\sqrt{2\pi r}} \cos\frac{\theta}{2} \left(1 + \sin\frac{\theta}{2} \sin\frac{3\theta}{2}\right) \\ \tau_{xy} &= \frac{K}{\sqrt{2\pi r}} \sin\frac{\theta}{2} \cos\frac{\theta}{2} \cos\frac{3\theta}{2} \end{aligned} \tag{1}$$

This representation (except for the $\sigma_{ox}$ term) is the exact solution for the case of the semi-infinite crack subject to biaxial loading. The $\sigma_{ox}$ term was subtracted from the expression for $\sigma_x$ to provide another degree of freedom so that the analytically determined fringe loop could be brought into closer correspondence with the experimentally observed loop.

The maximum shear stress $\tau_m$ is expressed in terms of the cartesian stress components as:

$$(2\tau_m)^2 = (\sigma_y - \sigma_x)^2 + (2\tau_{xy})^2 \tag{2}$$

From eqs (1) and (2), it is apparent that

*J.M. Etheridge is associated with Naval Surface Weapons Center, White Oak, MD 20901. J.W. Dally is Professor, Department of Mechanical Engineering, College of Engineering, Glenn L. Martin Institute of Technology, University of Maryland, College Park, MD 20742.*

*Original manuscript submitted: February 25, 1976. Final version received: January 6, 1977.*

*This research represents partial fulfillment of the requirements for a PhD degree at the University of Maryland.*

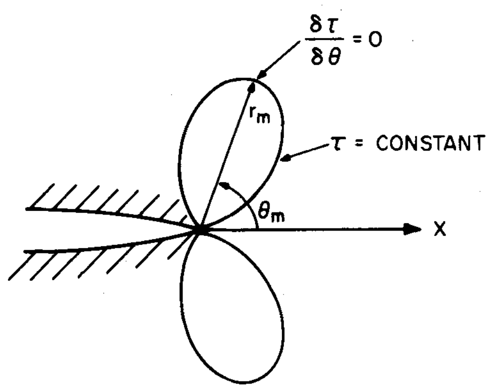


Fig. 1—Characteristic geometry of the isochromatic-fringe loop at the crack tip

$$(2\tau_m)^2 = \frac{K^2}{2\pi r}\sin^2\theta + \frac{2\sigma_{ox}K}{\sqrt{2\pi r}}\sin\theta\sin\frac{3\theta}{2} + \sigma_{ox}{}^2 \quad (3)$$

Next, Irwin observed the geometry of the fringe loops and noted that:

$$\frac{\partial\tau_m}{\partial\theta} = 0 \quad (4)$$

at the extreme position on the fringe loop where $r = r_m$ and $\theta = \theta_m$. Differentiating eq (3) with respect to $\theta$ and using eq (4) gives

$$\sigma_{ox} = \frac{-K}{\sqrt{2\pi r_m}}\,\frac{\sin\theta_m\cos\theta_m}{(\cos\theta_m\sin\frac{3\theta_m}{2} + \frac{3}{2}\sin\theta_m\cos\frac{3\theta_m}{2})} \quad (5)$$

The two unknown parameters $K$ and $\sigma_{ox}$ are determined from the complete solution of eqs (3) and (5) as:

$$\sigma_{ox} = \frac{-2\tau_m\cos\theta_m}{\cos(3\theta_m/2)\,[\cos^2\theta_m + (9/4)\sin^2\theta_m]^{1/2}} \quad (6)$$

and

$$K = \frac{2\tau_m\sqrt{2\pi r_m}}{\sin\theta_m}\left[1 + \left(\frac{2}{3\tan\theta_m}\right)^2\right]^{-1/2}\left(1 + \frac{2\tan\frac{3\theta_m}{2}}{3\tan\theta_m}\right) \quad (7)$$

Results for the normalized stress parameter $(\sigma_o/2\tau_m)$ obtained from eq (6) are shown in Fig. 2 as a function of $\theta_m$ over the physically admissable range of $60 < \theta_m < 180$ deg. Similarly, results for the normalized stress-intensity factor $K/2\tau_m\sqrt{2\pi r_m}$ are shown in Fig. 3 as a function of $\theta_m$ over the range of $69.4 \leq \theta_m \leq 148.8$ deg where $K$ is positive.

To further establish the range of $\theta_m$ over which the Irwin method is applicable, an analysis of the central-crack problem (i.e., a crack of length $2a$ in an infinite plate with biaxial loading at the boundaries) was performed. In the analysis of the central-crack problem, the far-field stress perpendicular to the crack was $\sigma_y = \sigma$ (tensile) and the far-field stress parallel to the crack was $\sigma_x = (1 + \varkappa)\sigma$ where the constant $\varkappa$ was varied from $+2.0$ to $-4.75$. Stress parameters $\tau_m/\sigma$ and a stress ratio $\varkappa$ were selected and a corresponding normalized fringe-loop radii $r_m/a$ and tilt angles $\theta_m$ were determined as shown in Table 1. The parameter $\tau_m/\sigma$ is proportional to the fringe order $N$ associated with the loop since

$$\tau_m = \frac{Nf_\sigma}{2h} \quad (8)$$

where $f_\sigma$ is the material-fringe value
$h$ is the model thickness

Values of $\tau_m/\sigma$ of 2, 2.5 and 3 were used to generate analytical fringe loops of appropriate size.

Next, the normalized stress-intensity factor $K/2\tau_m\sqrt{2\pi r_m}$

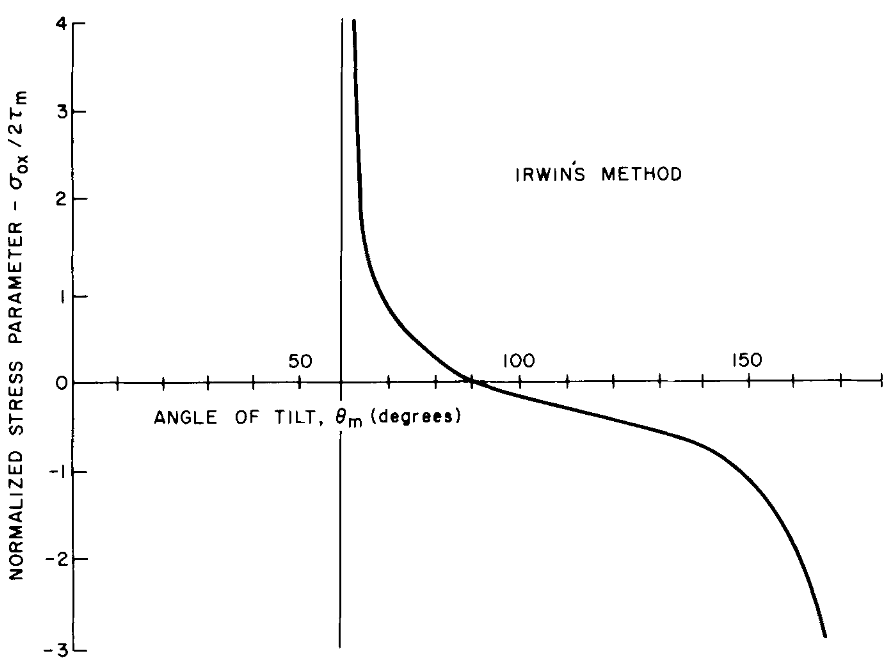


Fig. 2—Normalized stress parameter $(\sigma_{ox}/2\tau_m)$ as a function of tilt angle $\theta_m$

was computed from :

$$K/2\tau_m\sqrt{2\pi r_m} = 1/2(\tau_m/\sigma)\sqrt{4(r_m/2a)} \qquad (9)$$

since $K = \sqrt{\pi a}\,\sigma$ for the central-crack problem. This normalized stress-intensity factor is also shown in Table 1.

By using eq (7) together with the values of $r_m$ and $\theta_m$ from Table 1, it was possible to compute another normalized stress-intensity factor based on Irwin's two-parameter method. Comparison of the two normalized stress-intensity factors in Table 1 permit the error in the determination of $K$ to be evaluated. This error is shown as a function of $\theta_m$ in Fig. 4 for the different ratios of $\tau_m/\sigma$.

Inspection of Fig. 4 shows that the two-parameter method of Irwin will predict $K$ to within $\pm 5$ percent providing $73 < \theta_m < 139$ deg and to within $\pm 2$ percent providing $73.5 < \theta_m < 134$ deg. Outside these $\pm 5$ percent, the error increases rapidly and the two-parameter method is not applicable.

The size of the fringe loop relative to the crack length in this comparison is small. Inspection of Table 1 with $73 < \theta_m < 139$ deg shows that $r_m/a \leqslant 0.03$ for the larger angle and $r_m/a \leqslant 0.065$ for the smaller angle. The smaller the value of $r_m/a$ consistent with the precise measurement of $r_m$ gives more accurate predictions of $K$.

### *Bradley-Kobayashi Method*

Bradley and Kobayashi[4,7] modified Irwin's analysis by substituting the following expression for $\sigma_{ox}$ into eq (3)

$$\sigma_{ox} = \frac{\delta K}{\sqrt{\pi a}} \qquad (10)$$

where

$$\delta = \sigma_{ox}/\sigma \qquad (11)$$

and $\sigma$ is the far-field stress perpendicular to the crack. This substitution permits $K$ to be factored from eq (3) to give :

$$(2\tau_m)^2 = \frac{K^2}{2\pi r}\left(\sin^2\theta + 2\delta\sqrt{\frac{2r}{a}}\sin\theta\sin\frac{3\theta}{2} + \frac{2r\delta^2}{a}\right) \qquad (12)$$

Differentiating eq (12) with respect to $\theta$ and using eq (4) gives

$$\delta\sqrt{\frac{2r_m}{a}} = \frac{-\sin\theta_m\cos\theta_m}{\cos\theta_m\sin\frac{3\theta_m}{2} + \frac{3}{2}\sin\theta_m\cos\frac{3\theta_m}{2}} \qquad (13)$$

Then, substitution of eq (13) into eq (12) leads to :

$$K = \frac{\pm\sqrt{2\pi r_m}\,(2\tau_m)}{\sin\theta_m}\left(1 + \frac{2\tan\frac{3\theta_m}{2}}{3\tan\theta_m}\right)\left[1 + \left(\frac{2}{3\tan\theta_m}\right)^2\right]^{-1/2} \qquad (14)$$

where the plus sign is selected when $69.4 < \theta_m < 148.8$.

Comparison of eqs (7) and (14) shows that the Bradley-Kobayashi method is identical to the Irwin method in predicting $K$ from photoelastic data.

The Bradley-Kobayashi method gives the appearance of being a three-parameter method since eq (10) for $\sigma_{ox}$ contained both $\delta$ and $\sqrt{a}$ in addition to $K$. However, the two parameters $\delta$ and $a$ can be reduced to a single parameter by letting

TABLE 1—COMPARISON OF THE NORMALIZED STRESS-INTENSITY FACTOR

| $\tau_m/\sigma$ | $\theta_m$ (degrees) | $r_m/a$ | $\frac{K^*}{2\tau_m\sqrt{2\pi r_m}}$ | $\frac{K^{**}}{2\tau_m\sqrt{2\pi r_m}}$ | $\frac{\Delta K}{K}$ (percent) |
|---|---|---|---|---|---|
| 3.0 | 143.47 | .250 | 0.46 | 0.24 | -91.7 |
| | 143.1 | .096 | 0.48 | 0.38 | -26.3 |
| | 140.04 | .042 | 0.66 | 0.57 | -15.8 |
| | 139.4 | .032 | 0.69 | 0.66 | - 4.5 |
| | 137.74 | .026 | 0.76 | 0.73 | - 4.1 |
| | 136.04 | .022 | 0.82 | 0.8 | - 2.5 |
| | 129.72 | .015 | 0.97 | 0.96 | - 1.0 |
| | 121.45 | .012 | 1.07 | 1.06 | - 0.9 |
| | 118.18 | .012 | 1.09 | 1.08 | - 0.9 |
| | 107.2 | .012 | 1.099 | 1.09 | - 0.8 |
| | 99.76 | .012 | 1.08 | 1.07 | - 0.9 |
| | 88.19 | .015 | 0.98 | 0.97 | - 1.5 |
| | 84.24 | .017 | 0.91 | 0.9 | - 1.1 |
| | 79.92 | .022 | 0.8 | 0.79 | - 1.3 |
| | 76.01 | .035 | 0.638 | 0.63 | - 1.3 |
| | 74.52 | .047 | 0.55 | 0.55 | 0 |
| | 73.21 | .065 | 0.45 | 0.46 | 2.2 |
| | 71.96 | .098 | 0.34 | 0.38 | 10.5 |
| | 71.29 | .125 | 0.27 | 0.33 | 18.2 |
| | 70.51 | .165 | 0.17 | 0.29 | 41.4 |
| | 69.53 | .226 | 0.02 | 0.25 | 92.0 |
| 2.5 | 142.06 | .101 | 0.55 | 0.44 | -25.0 |
| | 140.69 | .063 | 0.62 | 0.56 | -10.7 |
| | 139.02 | .046 | 0.70 | 0.66 | - 6.1 |
| | 137.08 | .035 | 0.78 | 0.75 | - 4.0 |
| | 134.91 | .029 | 0.85 | 0.83 | -2.4 |
| | 129.76 | .022 | 0.92 | 0.9 | -2.2 |
| | 111.21 | .017 | 0.97 | 0.96 | -1.5 |
| | 102.21 | .017 | 1.02 | 1.01 | -1.5 |
| | 90.86 | .02 | 1.01 | 1.00 | -1.5 |
| | 83.45 | .026 | 0.89 | 0.88 | -1.1 |
| | 78.72 | .036 | 0.76 | 0.75 | -1.3 |
| | 76.44 | .047 | 0.66 | 0.65 | -1.5 |
| | 74.57 | .066 | 0.55 | 0.55 | 0 |
| | 73.74 | .08 | 0.49 | 0.5 | 2.0 |
| | 72.92 | .099 | 0.43 | 0.45 | 4.4 |
| | 72.11 | .126 | 0.35 | 0.4 | 12.5 |
| | 71.19 | .166 | 0.25 | 0.35 | 28.6 |
| | 70.62 | .200 | 0.18 | 0.32 | 43.8 |
| 2.0 | 140.43 | .110 | 0.64 | 0.53 | -20.8 |
| | 138.42 | .070 | 0.73 | 0.67 | - 9.0 |
| | 135.96 | .052 | 0.82 | 0.78 | - 5.1 |
| | 133.12 | .041 | 0.9 | 0.87 | - 3.4 |
| | 129.82 | .035 | 0.97 | 0.95 | - 2.1 |
| | 121.76 | .028 | 1.07 | 1.05 | - 1.9 |
| | 111.59 | .026 | 1.10 | 1.09 | - 0.9 |
| | 95.61 | .029 | 1.05 | 1.04 | - 1.5 |
| | 84.85 | .038 | 0.92 | 0.90 | - 2.0 |
| | 78.66 | .057 | 0.76 | 0.74 | - 3.0 |
| | 77.17 | .068 | 0.69 | 0.68 | - 1.5 |
| | 74.65 | .101 | 0.56 | 0.56 | 0 |
| | 73.5 | .128 | 0.48 | 0.49 | 2.0 |
| | 72.33 | .168 | 0.37 | 0.43 | 14.0 |
| | 71.0 | .229 | 0.23 | 0.37 | 37.8 |

* Irwin's two parameter method

** Exact, from the central crack problem

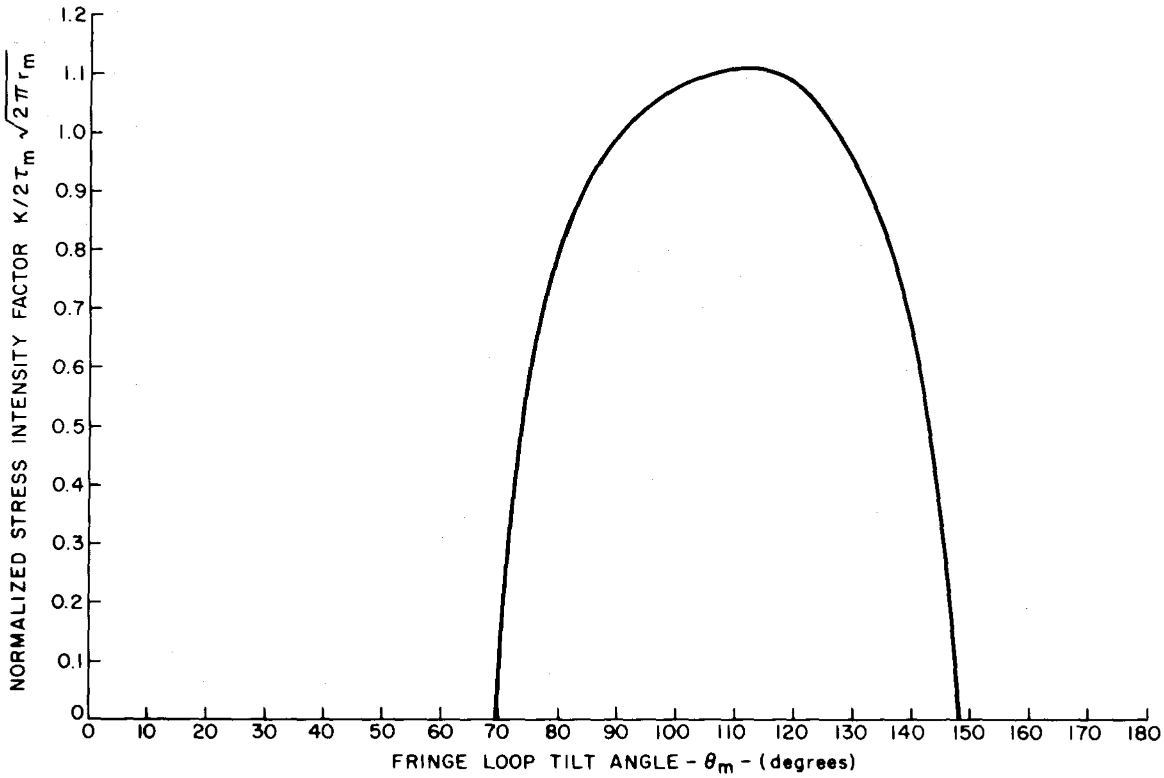


Fig. 3—Normalized stress-intensity factor $K/2\tau_m\sqrt{2\pi r_m}$ as a function of tilt angle $\theta_m$

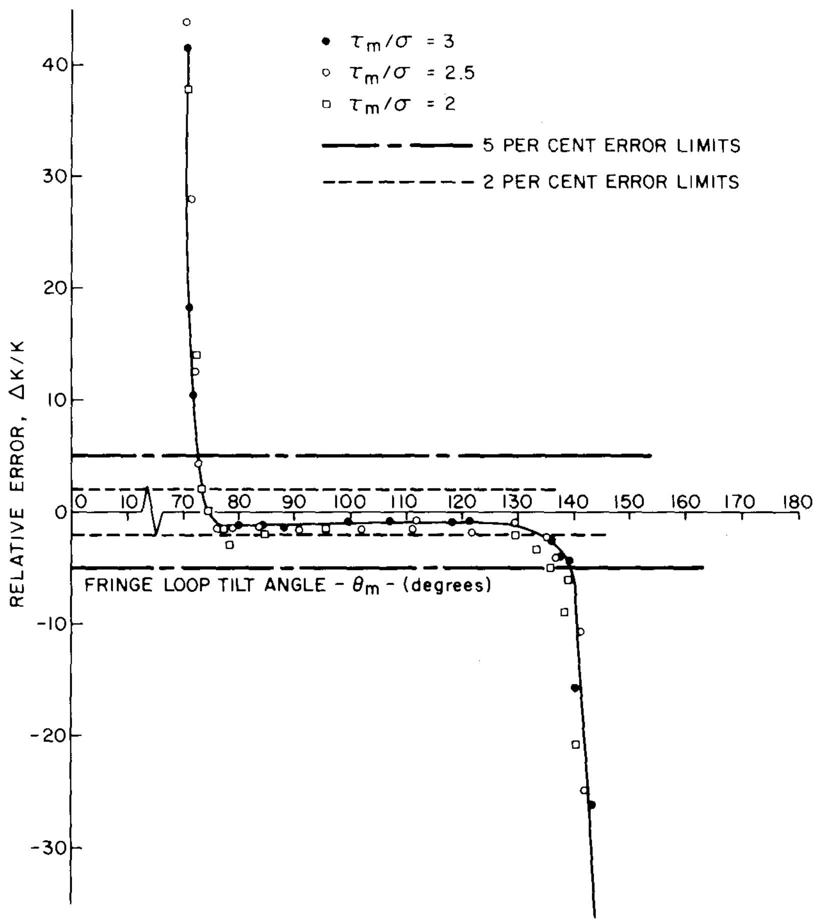


Fig. 4—Relative error as a function of tilt angle $\theta_m$ for Irwin's two-parameter method

$$\delta' = \delta/\sqrt{a} \tag{15}$$

Then eq (10) becomes

$$\sigma_{ox} = \delta' K/\sqrt{\pi} \tag{16}$$

Substituting eq (15) and eq (13) into eq (16) gives

$$\sigma_{ox} = \frac{-K}{\sqrt{2\pi r_m}} \frac{\sin\theta_m \cos\theta_m}{(\cos\theta_m \sin\frac{3\theta_m}{2} + \frac{3}{2}\sin\theta_m \cos\frac{3\theta_m}{2})} \tag{17}$$

Comparison of eq (17) and eq (6) shows that the Bradley-Kobayashi fitting parameter $\sigma_{ox}$ is identical to the Irwin $\sigma_{ox}$ and that the two methods are exactly the same.

Bradley and Kobayashi were concerned with errors produced in determining $K$ when $\theta_m$ was close to either 69.4 or 148.8. In these regions, small errors in measuring $\theta_m$ produce large errors in $K$. In order to minimize these errors Bradley and Kobayashi used two fringe loops with eq (12) to obtain :

$$K = 2\sqrt{2\pi}\sqrt{r_1 r_2}\,(\tau_2 - \tau_1)/(f_2\sqrt{r_1} + f_1\sqrt{r_2} \tag{18}$$

where

$$f = [\sin^2\theta + 2\delta\sqrt{2r/a}\sin\theta\sin(3\theta/2) + 2r\delta^2/a]^{1/2} \tag{19}$$

It is of interest to note the variation of the Bradley-Kobayashi normalized stress parameter $\delta\sqrt{2r_m/a}$ which is shown as a function of $\theta_m$ in Fig. 5. The parameter $\delta\sqrt{2r_m/a}$ is small (i.e. less than 0.2) for $82 < \theta_m < 113$ deg; however, the term cannot be neglected in comparison to $\sin^2\theta_m$ in computing $f$ from eq (19).

The value of $\delta\sqrt{2r_m/a}$ is relatively insensitive to small changes in $\theta_m$ over this range of tilt angle. This result confirms the observation by Bradley and Kobayashi that small changes in $\delta$ do not markedly affect $K$ for $90 < \theta_m < 120$ deg. Kobayashi and his associates[8,9] often simplify eq (19) by setting $\delta = 1$ when applying this differencing technique; however, this simplification has never been justified.

TABLE 2—THEORETICAL FRINGE-LOOP GEOMETRY

$Kh/f_\sigma = 1.535\sqrt{in}$ $(7.736\sqrt{mm})$, $a = 3$ in (76.2 mm)

| Fringe Order, N | $\sigma/\tau_m$ | $x$ | $r_m$ (in.) | $r_m$ (mm) | $\theta_m$ deg | r at $\theta = \pi/2$ (in.) | r at $\theta = \pi/2$ (mm) |
|---|---|---|---|---|---|---|---|
| 1 | 1 | 0.0 | 0.3757 | 9.54 | 93.59 | 0.3775 | 9.46 |
| 2 | 1/2 | 0.0 | 0.0938 | 2.38 | 90.92 | 0.0935 | 2.36 |

### *Schroedl-Smith Method*

Schroedl and Smith[5] determine the fringe order of the isochromatic loops along the line defined by $\theta = 90$ deg, and accordingly eq (3) reduces to :

$$(2\tau_m)^2 = \frac{K^2}{2\pi r^2} + \frac{K\sigma_{ox}}{\sqrt{2\pi r}} + \sigma_{ox}^2 \tag{20}$$

Solving eq (20) for $K$ and retaining only the positive root from the quadratic formula gives

$$K = \sqrt{\pi r}\,[(8\tau_m^2 - \sigma_{ox}^2)^{1/2} - \sigma_{ox}] \tag{21}$$

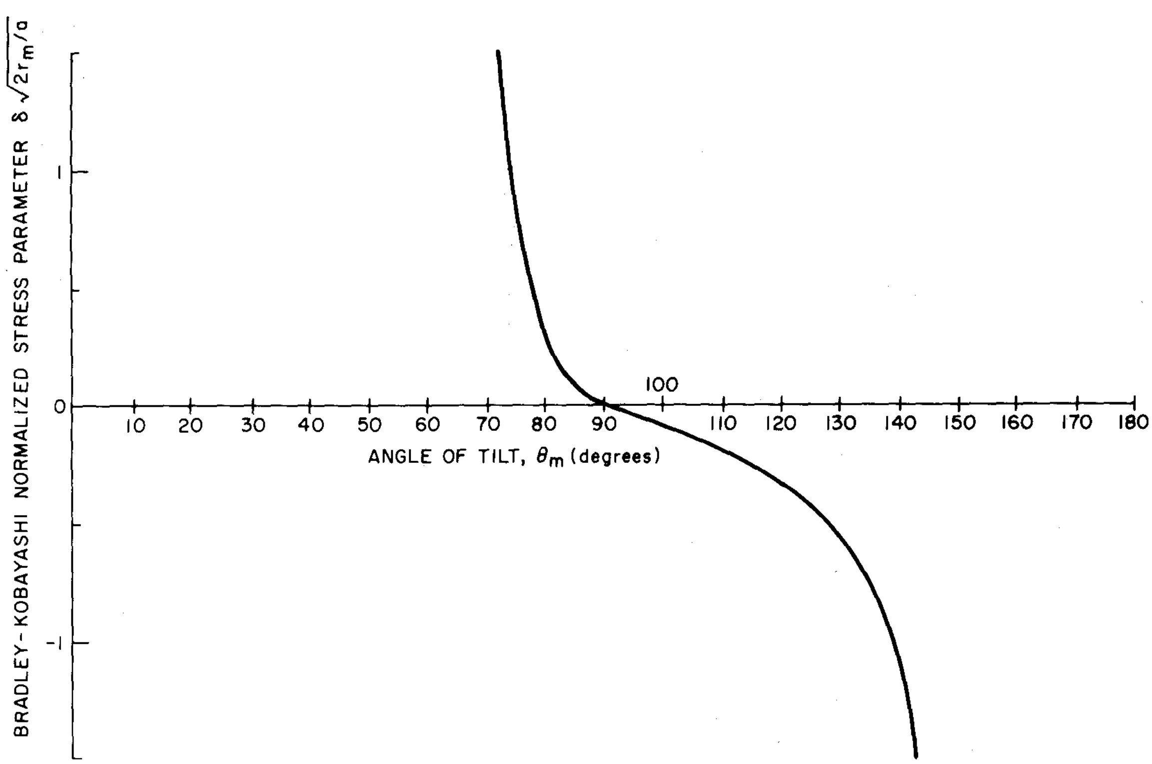


Fig. 5—Bradley-Kobayashi normalized stress parameter $\delta\sqrt{2r_m/a}$ as a function of tilt angle $\theta_m$

TABLE 3—COMPARISON OF THE TWO-PARAMETER METHODS FOR DETERMINING THE STRESS-INTENSITY FACTOR

| Method | N | Eq No. | $(Kh/f_\sigma)$* | $\Delta K/K$ (percent) |
|---|---|---|---|---|
| Irwin | 2 | 7 | 1.5546 | 1.28 |
| Irwin | 1 | 7 | 1.5912 | 3.68 |
| B-K | 1 and 2 | 18 | 1.5331 | −0.12 |
| S-S | 1 and 2 | 23 | 1.5278 | −0.47 |

* Exact value of $(Kh/f_\sigma)$ = 1.5350

Smith simplified eq (21) by neglecting $\sigma_{ox}^2$ relative to $8\tau_m^2$ to obtain

$$K = \sqrt{\pi r}\,[\sqrt{2}\,(2\tau_m) - \sigma_{ox}] \tag{22}$$

By adopting the Bradley-Kobayashi differencing technique, Smith uncouples the $K$ and $\sigma_{ox}$ relation. Using $\tau_m$ from the $i^{th}$ and $j^{th}$ fringe loops gives

$$K = \sqrt{2\pi r_i}\,\frac{(2\tau_m)_i - (2\tau_m)_j}{1 - \left(\frac{r_i}{r_j}\right)^{1/2}} \tag{23}$$

Smith and Schroedl compute $K$ from eq (23) for all possible permutations of pairs of fringe loops and from these values of $K$ they determine the average and standard deviation. The values of $K$ outside ± one standard deviation limits are eliminated and $K_{ave}$ is recomputed from the remaining values of $K$. The accuracy of this method has been discussed[10] and prediction of $K$ to ±5 percent is anticipated if the fringe loop radii $r_i$ and $r_j$ are measured without error.

## Comparison of the Three Methods

The results from an exact analysis of the central-crack problem provided the analytical basis for comparing the three methods. Two theoretical fringe loops, with $N = 1$ and 2, were generated for a crack length $2a = 6$ in (152 mm). In this case, $Kh/f_\sigma$ was taken as 1.535 $\sqrt{\text{in.}}$ (7.736 $\sqrt{\text{mm}}$) to give $\sigma N/\tau_m = 1$. The geometry parameters describing these loops $r_m$ and $\theta_m$ and $r$ at $\theta = \pi/2$ are given in Table 2.

These parameters were used in eqs (7), (18) and (23) to compute $Kh/f_\sigma$ for the three methods as shown in Table 3.

The comparison of the results for $Kh/f_\sigma$ obtained by using the approximate methods of Irwin, Bradley and Kobayashi, and Schroedl and Smith, show that all three methods provide solutions which are very close to the exact value of $Kh/f_\sigma$. Provided that no errors are made in the measurements of $r_m$ and $\theta_m$, the Bradley and Kobayashi eq (18) predicts the most accurate values, the Schroedl-Smith method is slightly less accurate, and Irwin's method has the largest error when compared to the exact results from the central-crack problem.

The error introduced by Kobayashi's practice of setting $\delta = 1$, when using eq (12) to determine $K$ from a single

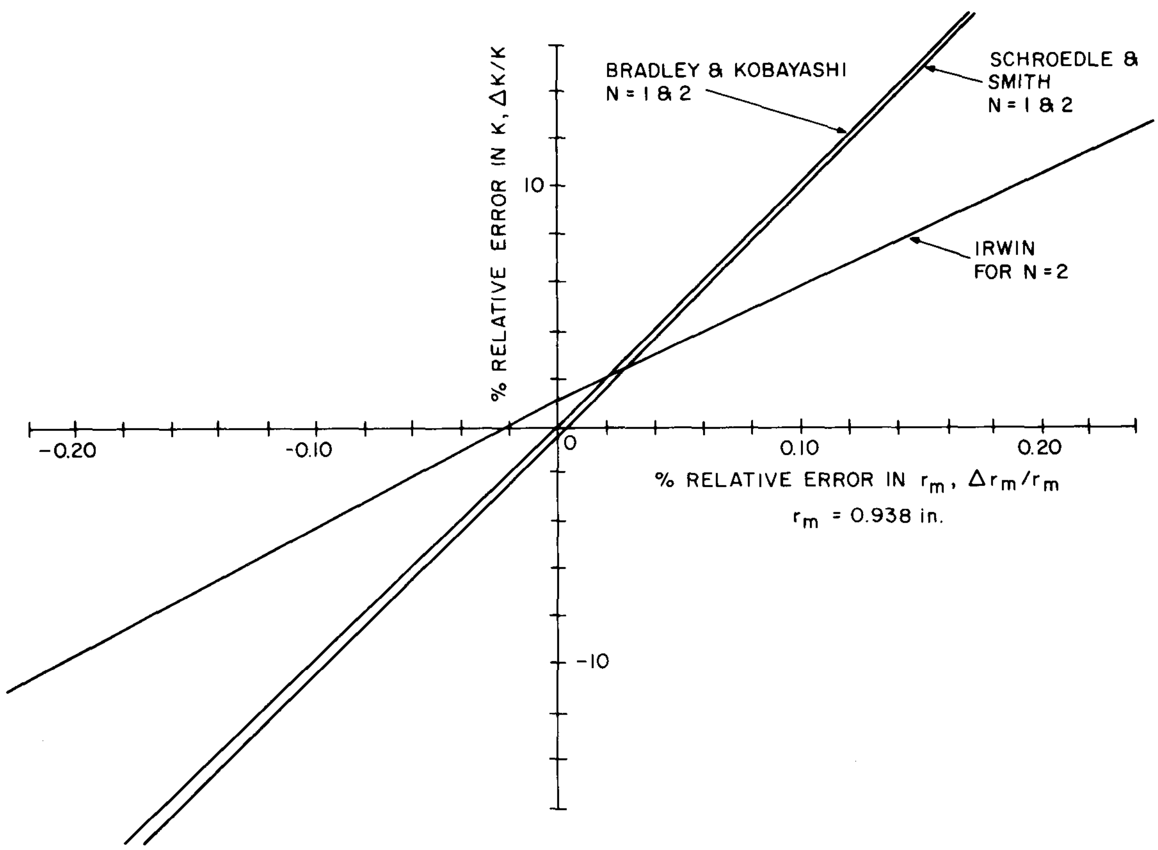


Fig. 6—Comparison of errors in $K$ as a function of measurement error $\Delta r_m$

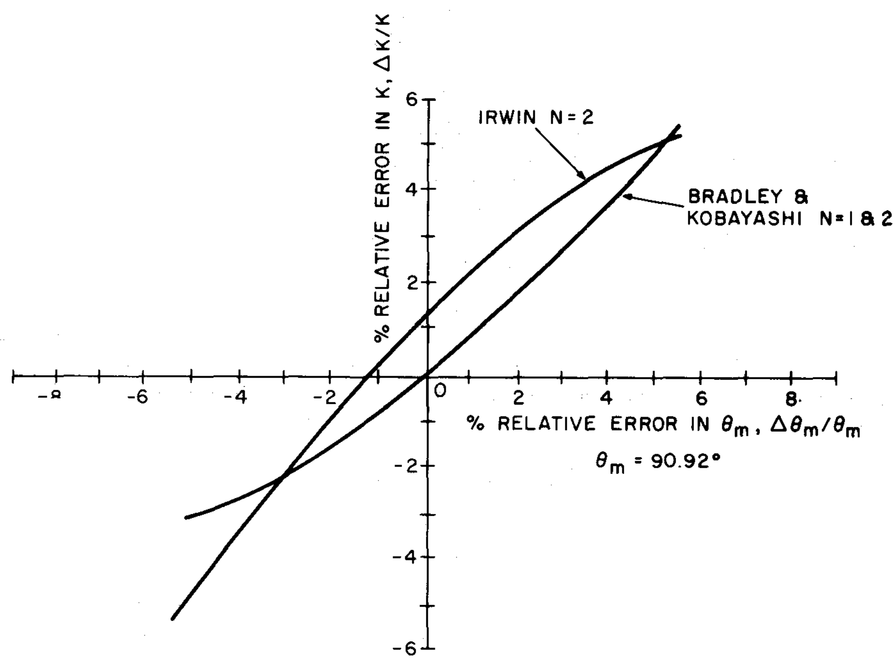


Fig. 7—Comparison of errors in $K$ as a function of measurement error $\Delta\theta_m$

fringe loop, was also evaluated using the data from Table 2. It was found that eq (12) gave $Kh/f_\sigma = 1.1194$ which is in error by $-27.07$ percent. Thus, it is evident that the simplification of eq (12) by setting $\delta = 1$ leads to significant errors in determining $K$.

If an error is made in the measurement of $r_m$, then an additional error results in determining $K$ for all three methods. The error in determining $K$ as a function of the deviation in the measurement $\Delta r_m$ of the $N = 2$ fringe is presented in Fig. 6 for the three different methods. It is evident from these results that the two differencing methods lead to larger errors since the differencing procedure amplifies the relative error.

If an error is made in the measurements of $\theta_m$, the methods of Irwin and Bradley and Kobayashi propagate this error as shown in Fig. 7. Irwin's method introduces more error for positive $\Delta\theta_m$ errors due to the initial positive error in $K$ when $\Delta\theta_m = 0$. For the same reason, Irwin's method introduces less error for negative $\Delta\theta_m$ errors providing $\Delta\theta_m > -3$ deg.

## Conclusions

The two-parameter methods are all applicable for determining $K$ in the range $73 < \theta_m < 139$ deg provided $r_m/a < 0.03$. If no measurement errors are made in $r_m$ or $\theta_m$, the two parameter methods will predict $K$ with an accuracy of $\pm$ 5 percent.

When two or more fringe loops occur at the crack tip and the radii can be measured with better than 2 percent accuracy, then the Bradley-Kobayashi shear-stress differencing method provides the most accurate results. When the measurement errors exceed 2 percent, the differencing technique magnifies these errors and Irwin's method produces more accurate estimates of $K$. The Irwin method is slightly more sensitive to errors in the measurement of $\theta_m$ than the Bradley-Kobayashi method.

The errors in $\theta_m$ determination can be eliminated in the differencing methods of Schroedl and Smith and Kobayashi and Bradley since any fixed value of $\theta$ can be employed. However, at least part of this advantage is offset by the error introduced in making the second $r$ measurement. (Note that the results of Fig. 6 are for an error introduced in only one $r$ measurement).

If only one fringe loop is available for analysis, Irwin's method must be used because it is the only method which can analyze a single fringe loop. Recall that the single-fringe-loop analysis obtained from the Bradley-Kobayashi method was shown to be identical with Irwin's method.

### Acknowledgments

J.M. Etheridge would like to express his appreciation to the Naval Surface Weapons Center for their support and encouragement. J.W. Dally would like to thank the Nuclear Regulatory Commission for their support of this program. Advice and comments by George R. Irwin have also been quite helpful in this review.

### References

1. Post, D., "Photoelastic Stress Analysis for an Edge Crack in a Tensile Field," Proc. of SESA, **12** (1), 99-116 (1954).
2. Wells, A. and Post, D., "The Dynamic Stress Distribution Surrounding a Running Crack—A Photoelastic Analysis," Proc. of SESA, **16** (1), 69-92 (1958).
3. Irwin, G.R., Disc. of Ref. 2, Proc. of SESA, **16** (1), 93-96 (1958).
4. Bradley, W.B., "A Photoelastic Investigation of Dynamic Brittle Fracture," PhD Thesis, Univ. of Washington (1969).
5. Schroedl, M.A. and Smith, C.W., "Local Stress Near Deep Surface Flaws Under Cylindrical Bonding Fields," Progress in Flaw Growth and Fracture Toughness Testing, ASTM STP 536, ATM, 45-63 (1973).
6. Irwin, G.R., "Analysis of Stresses and Strains Near the End of a Crack Traversing a Plate," J. Appl. Mech., **24** (3) (Sept. 1957).
7. Bradley, W.B. and Kobayashi, A.S., "An Investigation of Propagating Cracks by Dynamic Photoelasticity," EXPERIMENTAL MECHANICS, **10** (3), 106-113 (March 1970).
8. Kobayashi, A.S., Wade, B.G. and Bradley, W.B., "Fracture Dynamics of Homalite-100," Deformation and Fracture of High Polymers, Kausch, H.H., Haseell, J.A., Jaffee, R.I., eds., Plenum Press, New York, 487-500 (1973).
9. Kobayashi, A.S., Mall, S. and Lee, M.H., "Fracture Dynamics of Wedge-Loaded DCB Specimen," presented at ASTM Meeting, August 1975, Pittsburgh, PA, to be published.
10. Schroedl, M.A., McGowen, J.J. and Smith, C.W., "An Assessment of Factors Influencing Data Obtained by the Photoelastic Stress Freezing Technique for Stress Fields Near Crack Tips," VPI-E-72.6, J. of Engrg. Fract. Mech., **4** (4), 801-809 (Dec. 1972).